

Fig. 2. Schematic representation of the rhombic dodecahedron single-crystal sample of almandine-garnet used in this study.

a series of 5-mm-thick slabs oriented perpendicular to the [100] direction. External morphology was used as a reference for orientation, and the uncertainty in this parameter is estimated to be <3%. The central slab was selected to determine the composition of the sample. A series of nine microprobe analyses were made across the slab at approximately equal intervals. Each point was probed for Mg, Fe, Ca, Mn, Al, and Si (Figure 3). Minor 'zoning' in the proportions of the eightfold coordinated cations is evident. This feature is rather common in almandine-garnet and appears to reflect a general pattern of substitutions in the garnet molecule as a result of progressive metamorphism, FeO + MgO substituting for CaO + MnO with increasing metamorphic grade [Deer *et al.*, 1962]. However, because the densities of the individual target specimen blanks were quite consistent, the compositional deviations were regarded as negligible in the final data analyses. An average bulk composition of  $(\text{Fe}_{0.76}, \text{Mg}_{0.14}, \text{Ca}_{0.04}, \text{Mn}_{0.03})_3\text{Al}_2\text{Si}_3\text{O}_{12}$  was adopted for the garnet sample. This composition is consistent with the measured lattice parameter and the density within the experimental uncertainty.

In addition, several thin sections were cut from the middle section. These revealed a minimal occurrence of internal fractures and negligible alteration. The dominant mineral phase was optically isotropic almandine-garnet; however, a minor fraction of opaque grains was randomly disseminated throughout the garnet matrix. This mineral appeared as hexagonal platelets and amounted to somewhat less than 0.5% of the total volume. A microprobe analysis

of the individual inclusions revealed a high proportion of Ti and Fe, thus suggesting ilmenite ( $\text{FeTiO}_3$ ) as the most probable composition. Although this material is of no consequence as far as the shock compression data are concerned, it hampered the X ray examination of the shock recovery experiment. The index of refraction of the garnet was measured at  $1.802 \pm 0.003$  at  $24^\circ\text{C}$ . This value is consistent with the indicated composition.

The lattice parameter of the Salida garnet sample was determined by using the standard Debye-Scherrer powder diffraction method. Approximately 16 lines in the back reflection region were used in a  $\cos^2 \theta$  extrapolation to obtain a value of  $a = 11.519 \pm 0.001 \text{ \AA}$ . The density of the sample, calculated from this lattice parameter and the microprobe composition, is  $4.19 \pm 0.02 \text{ g/cm}^3$ . The estimated uncertainty in this case is primarily the result of possible error in the indicated composition rather than in the measured lattice parameter. This value is consistent with the range of measured bulk densities of the individual target specimens.

Because of the occurrence of minor inclusions of ilmenite ( $\text{FeTiO}_3$ ) in the Salida sample, recovery experiments were made on an additional

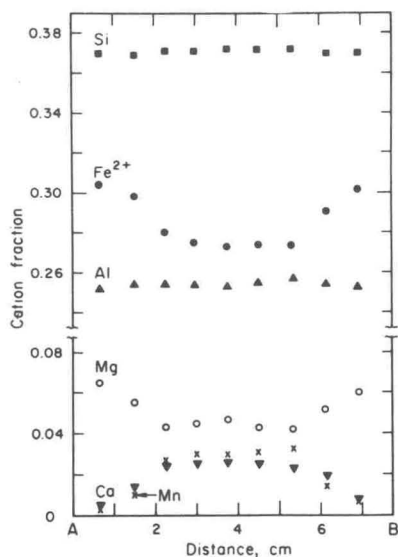


Fig. 3. Microprobe analyses of the points along the central almandine section. The line AB in Figure 2 indicates the approximate locus of sample points. Electron microprobe analyses were done by A. Chodos.



iron-rich garnet specimen (Brazil) that appeared in thin section to be completely free of included mineral impurities. After electron microprobe analysis, the particular sample selected proved to contain a significant proportion of the spessartine molecule in addition to almandine. The composition was determined to be  $(\text{Fe}_{0.52}, \text{Mn}_{0.47}, \text{Ca}_{0.01})_3 \text{Al}_2\text{Si}_2\text{O}_{12}$ , which is consistent with the measured density of  $4.247 \pm 0.001 \text{ g/cm}^3$  and the lattice parameter  $a = 11.572 \pm 0.001 \text{ \AA}$ . However, because of the similarity in the ionic radii of  $\text{Fe}^{2+}$  and  $\text{Mn}^{2+}$ , there is good reason to expect that the two garnet samples will transform into equivalent structures in the high-pressure regime.

Twenty-five specimen target blanks were cored from the oriented almandine slabs. The targets were cut as cylindrical disks 18 mm in diameter; the faces were finished flat and parallel to a thickness of approximately 5 mm. Individual target blanks were cored from areas of the oriented slabs that were most free from internal fracture and inhomogeneity as indicated by X ray radiography shadowgraphs. Bulk densities of the individual samples were measured by using the method of water immersion and are considered accurate to  $\pm 0.05\%$ . The range of densities varied from 4.175 to  $4.186 \text{ g/cm}^3$ , except for a single blank cored from the center of the original single crystal; the variation is attributable to the slight compositional zoning previously discussed. Successful Hugoniot high-pressure data were obtained for 18 of the original garnet target blanks. The initial density and the thickness of these individual samples are indicated in Table 1. Thicknesses were measured with a comparator and are accurate to within  $\pm 0.05\%$ .

#### SHOCK WAVE MEASUREMENTS

The experimental technique of generating and measuring shock waves in solids by using the Caltech high-performance gun has been described by Lower and Ahrens [1969] and Ahrens *et al.* [1970]. Only a brief description will be given here as being pertinent to the present problem.

The finished target blanks were mounted on 1.5-mm-thick driver plates that had been ground flat and parallel. Three types of driver plates were used: polycrystalline tungsten, density  $19.2 \text{ g/cm}^3$ ; tungsten alloy (fansteel),

density  $16.9 \text{ g/cm}^3$ ; and aluminum 2024, density  $2.79 \text{ g/cm}^3$ . Flat and inclined mirrors were placed on the sample and the driver plates to record shock arrivals at the sample-driver plate interface and at the sample free surface. The velocity of the planar shock wave through the sample was measured by recording the time between destructions of the mirror-reflecting coatings by using a xenon flash tube light source and an image converter (streak) camera [Ahrens *et al.*, 1970]. Calibration for the film records was provided by a pulsed argon laser that was intensity modulated by a Pockels cell to provide 50-nsec time marks. The primary source of error in the shock velocity determinations was a result of the uncertainty in the precise location of the various shock wave arrivals on the photographic records. As is indicated in Tables 1 and 2, the measured wave velocities are generally considered accurate to within  $\pm 0.5\%$ .

Shock pressures from about 100 to over 650 kb were induced in the garnet sample blanks by impacting a flyer plate onto the target assembly. The 3.5-mm-thick flyer plates were composed of the same material as the driver plates and were embedded in the ends of specially designed Lexan projectiles. The projectiles were fired at the targets at velocities between 0.8 and 2.5 km/sec by using the Caltech high-performance gun. Projectile velocities were measured along the last 50 cm of the 8-meter barrel by using a series of three He-Ne laser photodiode arrangements. Velocities of the flyer plates at impact, which were required for the impedance-matching method used in the Hugoniot state determinations, were generally better than  $\pm 1\%$ . Appropriate shock tilt corrections resulting from nonplanar impacts of the flyer driver plates were applied when necessary.

Final Hugoniot states have been determined for the 18 shock wave experiments by using the usual Rankine-Hugoniot equations and method of impedance matching [Rice *et al.*, 1958]. Because a double-wave structure was observed on the low-pressure data, the velocity of the second wave was corrected, when necessary, for the interaction of the refraction arising from the reflection of the first shock front at the free surface, according to the method suggested by Ahrens *et al.* [1968].